Helicity and isospin asymmetries in the electroproduction of nucleon resonances

M. Warns,* W. Pfeil, and H. Rollnik
Physikalisches Institut, Universität Bonn, D-5300 Bonn, West Germany
(Received 3 November 1989)

We investigate the helicity asymmetries and isospin ratios of radiative transition amplitudes for nucleon resonances electroproduced off proton and neutron targets at momentum transfers of $Q^2 \leq 3$ GeV^2. Calculations were done in the framework of a relativized constituent quark model which includes many-body effects due to the quark interaction potential and a consistent relativistic approximation of the center-of-mass motion of the three-quark system. We find significant deviations from the predictions of the nonrelativistic quark models and the SU(6)$_W$ algebraic approach based on the single-quark-transition hypothesis. Our calculated relativistic corrections lead to an overall better agreement with the experimental data. The question of whether some of the low-lying P-wave baryons are of hybrid nature is briefly discussed. Finally we analyze the electroexcitation of the missing $(20,1^+)$ P-wave resonances.

I. INTRODUCTION

With the new generation of electron accelerators CEBAF, ELSA in Bonn, and MAMI in Mainz becoming operational, the precise study of elastic and inelastic electron-nucleon scattering up to momentum transfers $Q^2 \leq 5$ GeV^2 will become possible. Experiments of this type are especially suited for a detailed study of the nonperturbative aspects of quantum chromodynamics (QCD). At low- and medium-energy transfers, the cross sections for these reactions are dominated by the excitation of various nucleon resonances. Since the photon is a spin-1 particle with isoscalar and isovector components, one gets a rich structure by varying the target polarization and by choosing proton or neutron targets for the experiments. Unfortunately due to their nonperturbative nature, one has not been able until now to calculate the resonance electroexcitation amplitudes directly from the QCD Lagrangian. On the other hand, there exist nowadays different "QCD-motivated" models leading to quantitative results for these amplitudes which have to be compared with the data. Using ratios or linear combinations of the different amplitudes may then help to factor out common model-dependent effects and thereby to test more general features such as selection rules, sum rules, and the connection with the high-Q^2 regime where perturbative QCD calculations start to become reliable. The first complete set of predictions for these amplitudes has been derived in the framework of the algebraic SU(6)$_W$ approach (for a review see, e.g., Ref. 1). Among the different dynamical models, the nonrelativistic constituent quark model (NRQM) elaborated by Isgur and collaborators (see, e.g., Ref. 2) gave the most complete set of photoproduction amplitudes. Recently, we have presented[3] a relativization of this model including multiquark effects originating from the quark interaction potential and the recoil motion during the photon-baryon scattering process. Our results for the electroproduction amplitudes of proton resonances (see Ref. 4) show significant differences in comparison to the nonrelativistic ansatz and lead to an improved agreement with the experimental data up to the limit of validity of our model, i.e., $Q^2 \approx 3$ GeV^2.

The purpose of this paper is to show how far some predictions made by the NRQM for the helicity and isospin asymmetries at $Q^2=0$ are modified by the relativistic corrections included in our model. This relativization permits us to extend these predictions to the electroproduction region up to $Q^2 \approx 3$ GeV^2. We complete our previous results by some relevant neutron radiative transition amplitudes. In this context, the electroexcitation of hybrid baryons and the experimentally still undetected nucleon resonances belonging to the $(20,1^+)$ multiplet are also discussed.

II. BRIEF DESCRIPTION OF THE MODEL

Before describing our results, it may be helpful to review the main features of our model especially in comparison with the nonrelativistic ansatz (a detailed description of the model can be found in Ref. 3). We consider only throughout this paper the electroexcitation by transversely polarized virtual photons. The nonrelativistic photon-baryon interaction Hamiltonian is in this case given by

$$H^{(0)} = \sum_{j=1}^{3} H_j^{(0)} , \tag{2.1}$$

$$H_j^{(0)} = -\frac{e_j}{2m_j c}[\mathbf{p}_j \cdot \mathbf{A}(\mathbf{r}_j) + \mathbf{A}(\mathbf{r}_j)\cdot \mathbf{p}_j + i\sigma_j \cdot \mathbf{k} \times \mathbf{A}(\mathbf{r}_j)] , \tag{2.2}$$

where the quark of number j at position $\mathbf{r}_j$ has charge e_j, mass m_j, and momentum $\mathbf{p}_j$, and $\mathbf{k}$ is the three-momentum of the photon ($k=(k^0,\mathbf{k}), k^2=-Q^2$). This Hamiltonian is a sum of single-quark interaction terms. We restrict ourselves in this paper to baryons consisting of u and d quarks. Assuming SU(2)-flavor symmetry (i.e., constituent quark masses $m_u = m_d$) it is sufficient to consider the Hamiltonian (2.2) describing the interaction of a

free quark (e.g., No. 3) with the photon and to multiply the result by 3 in order to get the final Hamiltonian for the baryon:

$$H^{(0)}=3H_3^{(0)} \ . \tag{2.3}$$

On account of the parity conservation in electromagnetic interactions, the Hamiltonian (2.2) is completely determined by considering a photon with helicity $+1$ traveling along the z axis [i.e., $A^\mu=(A^0=0, A^-, A^z=0)$; $k^\mu=(k^0, k^x=k^y=0, k^z=|\mathbf{k}|)$]:

$$H_3^{(0)}=e_3 \mathcal{J}_3^{(0)^+} A^-(\mathbf{r}_3) \ , \tag{2.4}$$

where we have introduced spherical coordinates for the electromagnetic vector potential $\mathbf{A}$:

$$A^\pm(\mathbf{r}):=\mp\frac{1}{\sqrt{2}}[A^x(\mathbf{r})\pm iA^y(\mathbf{r})] \ .$$

$\mathcal{J}_3^{(0)}$ is the nonrelativistic quark current operator, i.e., a 2×2 matrix in the spin space of the third quark. The decomposition of $\mathcal{J}_3^{(0)+}$ in terms of the SU(2) spin generators $\{\mathbb{1},\boldsymbol{\sigma}_3\}$ can be written in the form

$$\mathcal{J}_3^{(0)^+}=\mathcal{A}^+\mathbb{1}+\mathcal{B}^z\sigma_3^+ \ . \tag{2.5}$$

The superscripts on the operators $\mathcal{A},\mathcal{B}$ denote their transformation properties under spatial rotations; e.g., $\mathcal{A}^+$ transforms as the L^+ component of the angular momentum. However the most general decomposition of a single-quark current operator in spin space reads[5]

$$\mathcal{J}_3^{\mathrm{SQ}^+}=\mathcal{A}^+\mathbb{1}+\mathcal{B}^z\sigma_3^+ +\mathcal{C}^+\sigma_3^z+\mathcal{D}^{++}\sigma_3^- \ . \tag{2.6}$$

The last two terms occur if one requires the usual transformation properties of the electromagnetic current operator component $\mathcal{J}^+$ under rotation. This general form can also be obtained in the framework of the algebraic $\mathrm{SU}(6)_W$ approach from the connection between current and constituent quarks via a Melosh transformation.[6,7] Because of this underlying symmetry group, the electroproduction amplitudes can be calculated using expression (2.6) in terms of Clebsch-Gordan factors and reduced matrix elements (for a review see, e.g., Refs. 5, 8, and 9).

In the framework of the NRQM, the term $\mathcal{C}^+\sigma_3^z$ (often referred to as a "spin-orbit" term) is obtained as a relativistic correction to the Hamiltonian (2.2) by performing a Foldy-Wouthuysen expansion[10] of the relativistic free quark-photon interaction (see, e.g., Ref. 11 for details).

However, at this stage relativistic effects arise also from the fact that the interacting quark is bound with two other partners inside a baryon. First of all the quark-quark interaction potential not only introduces configuration mixing in the nonrelativistic wave functions but also leads to additional terms in the interaction Hamiltonian. Furthermore, the relativistic center-of-mass motion of the three-quark system has also to be treated in a systematic way. In our model,[3] we have derived in a consistent manner these additional terms for the electromagnetic interaction Hamiltonian by expanding the corresponding relativistic expressions in powers of the quark velocity $|\mathbf{p}|/m_q$. The Hamiltonian obtained contains in the lowest order the nonrelativistic part (2.1) and additional terms of order $(|\mathbf{p}|/m_q)^2$ related to the relativistic effects mentioned above. Our final result for the current operator reads, in a generalization of the notation introduced previously,

$$\mathcal{J}_3^+=\mathcal{A}^+\mathbb{1}+\mathcal{B}^z\sigma_3^+ +\mathcal{C}^+\sigma_3^z+\mathcal{D}^{++}\sigma_3^- \tag{2.7a}$$

$$+\mathcal{B}_\lambda^z\sigma_\lambda^+ +\mathcal{C}_\lambda^+\sigma_\lambda^z+\mathcal{D}_\lambda^{++}\sigma_\lambda^- \tag{2.7b}$$

$$+\mathcal{B}_\rho^z\sigma_\rho^+ +\mathcal{C}_\rho^+\sigma_\rho^z+\mathcal{D}_\rho^{++}\sigma_\rho^- \tag{2.7c}$$

$$+\mathcal{C}_{3\lambda}^+\sigma_3^+\sigma_\lambda^- +\mathcal{C}_{3\rho}^+\sigma_3^+\sigma_\rho^- +\mathcal{E}_{3\lambda}^-\sigma_3^+\sigma_\lambda^+ +\mathcal{E}_{3\rho}^-\sigma_3^+\sigma_\rho^+ \ , \tag{2.7d}$$

where the additional terms (2.7b)–(2.7d) describe two- and three-particle interactions which enter through the spin matrices

$$\boldsymbol{\sigma}_\lambda=\tfrac{1}{2}(\boldsymbol{\sigma}_1+\boldsymbol{\sigma}_2), \quad \boldsymbol{\sigma}_\rho=\tfrac{1}{2}(\boldsymbol{\sigma}_1-\boldsymbol{\sigma}_2) \ .$$

Since the photon was coupled to the third quark in deriving this expression, the additional terms (2.7b)–(2.7d) represent the recoil effects of the photon-quark interaction on the two other quarks inside the baryon. Especially the $\mathcal{D}^{++}$ terms and the last part (2.7d) occur only by treating the center-of-mass motion of the three-quark system in a consistent relativistic approximation. The various operators $\mathcal{A},\mathcal{B},\ldots$ acting on the spatial part of the wave functions depend also on the forces between the quarks inside the baryon and violate the simple $\mathrm{SU}(6)_W$ symmetry used in the derivation of (2.6).

The total electromagnetic interaction Hamiltonian is then built up in analogy to Eqs. (2.3) and (2.4):

$$\mathcal{H}_{\mathrm{em}}^+=3e_3\mathcal{J}_3^+A^-(\mathbf{r}_3) \ . \tag{2.8}$$

This operator can now be used to calculate the electromagnetic transition amplitudes between the target nucleon and the excited resonance. To compute the corresponding matrix elements, we used the harmonic-oscillator wave functions calculated by Isgur and coworkers[12] in the framework of the NRQM. The configuration mixing arising from the hyperfine interaction is included as a further relativistic correction in our model on the same footing as the other effects. These wave functions are obviously not eigenstates of our Hamiltonian but we used them (as motivated in Ref. 3) as a first-order approximation. This procedure is supported by the fact that the relativistic effects included in our Hamiltonian modify the nonrelativistic results only by an amount of less than 30%.

The parameters occurring in our model have been fixed as follows. The quark masses, oscillator strength, and mixing angles of the wave functions are taken from the work of Isgur *et al.*[12] For the potential describing the interaction between the quarks we took an ansatz composed of a scalar and a Lorentz-vector part. In our opinion up to now the shape of these potentials has not been definitely determined by quark-model calculations of the mass spectrum (for an excellent review of the present situation see Ref. 13). Therefore we decided to fix their parametrizations by fitting the experimental data of

the electromagnetic nucleon form factors and the electromagnetic transition amplitudes of higher isobars belonging to multiplets with nonvanishing angular momentum. For a detailed discussion of the resulting potentials we refer to our previous publication.[4]

The helicity amplitudes to be considered in the following are defined in the standard fashion according to Ref. 14 (see Ref. 4 for details and conventions):

$$A^N_{1/2}=\left[\frac{4\pi\alpha}{2K_W}\right]^{1/2}\langle\Psi_{N^*},J_z=\tfrac{1}{2}|\mathcal{H}^+_{\rm em}|\Psi_N,S_z=-\tfrac{1}{2}\rangle\xi\ , \tag{2.9}$$

$$A^N_{3/2}=\left[\frac{4\pi\alpha}{2K_W}\right]^{1/2}\langle\Psi_{N^*},J_z=\tfrac{3}{2}|\mathcal{H}^+_{\rm em}|\Psi_N,S_z=\tfrac{1}{2}\rangle\xi\ , \tag{2.10}$$

where the index $N=p,n$ refers to the target nucleon (proton, neutron of spin S and mass M), ξ is the sign of the decay amplitude of the resonance N^* (spin J, mass W) in the πN channel, K_W means the photon energy in the center-of-mass frame,

$$K_W=\frac{W^2-M^2}{2W}\ , \tag{2.11}$$

and $\alpha=\frac{1}{137}$ is the fine-structure constant. The reference frame chosen to calculate the matrix elements is the "equal velocity" frame (EVF) where the incoming nucleon and outgoing resonance have opposite velocities:

$$\frac{\mathbf{P}_{\rm in}}{M}=-\frac{\mathbf{P}_{\rm out}}{W}\ . \tag{2.12}$$

The results for the photoproduction ($Q^2=0$) amplitudes of all nucleon resonances discussed in this paper are collected in Table I. Some of the corresponding electroexcitation ($Q^2>0$) amplitudes have already been presented in our previous publication;[4] the remaining ones can be taken from the graphs included in this paper.

III. HELICITY ASYMMETRIES

The helicity asymmetries are defined by the expression

$$A^N:=\frac{|A^N_{1/2}|^2-|A^N_{3/2}|^2}{|A^N_{1/2}|^2+|A^N_{3/2}|^2}\ . \tag{3.1}$$

In the limit $Q^2\to\infty$ perturbative QCD calculations[18] predict hadron helicity conservation in exclusive processes which here means that the ratio $A^N_{3/2}/A^N_{1/2}$ vanishes and therefore leads to

$$A^N(Q^2\to\infty)=1\ . \tag{3.2}$$

On the other hand if one looks at the available experimental resonance photoproduction ($Q^2=0$) data displayed in Table I the low-lying nucleon resonances

TABLE I. Calculated photoproduction amplitudes of various nucleon resonances in units of 10^{-3} GeV$^{-1/2}$. For comparison the experimental data and the results calculated with the nonrelativistic quark model including configuration mixing (column NRQM) are presented.

Resonance multiplet	Amplitude	Experimental data Ref. 15	Ref. 16	Ref. 17	NRQM	Our model Ref. 3
$P_{33}(1232)$	$A^{p,n}_{3/2}$	−264±2	−259±6	−247±10	−163	−170
$(56,0^+)0$	$A^{p,n}_{1/2}$	−147±1	−138±4	−136±6	−93	−81
$P_{11}(1470)$	$A^p_{1/2}$	−68±15	−69±4	−63±8	−105	−9
$(56,0^+)2$	$A^n_{1/2}$	23±9	37±10	56±15	70	0.5
$S_{11}(1535)$	$A^p_{1/2}$	83±7	77±21	65±16	116	54
$(70,1^-)2$	$A^n_{1/2}$	−75±9	−35±14	−98±26	−93	−57
$D_{13}(1520)$	$A^p_{3/2}$	167±10	178±3	168±13	65	63
$(70,1^-)2$	$A^p_{1/2}$	−19±7	−32±5	−7±4	−79	−7
	$A^n_{3/2}$	−147±8	−124±9	−144±15	−75	−118
	$A^n_{1/2}$	−76±6	−66±13	−56±11	8	−36
$P_{11}(1710)$	$A^p_{1/2}$	−9±6	28±9	15±25	56	−8
$(70,0^+)2$	$A^n_{1/2}$	11±21	0±18	−17±20	−23	≈0
$F_{15}(1680)$	$A^p_{3/2}$	115±8	115±8	141±14	55	87
$(56,2^+)2$	$A^p_{1/2}$	−28±9	−9±6	−18±14	−68	18
	$A^n_{3/2}$	−24±9	−33±13	−33±15	−13	−18
	$A^n_{1/2}$	26±5	17±14	44±12	50	−4
$P_{13}(1730)$	$A^p_{3/2}$	−58±26	−40±16	−14±40	−22	−14
$(56,2^+)2$	$A^p_{1/2}$	51±25	−4±7	38±50	120	69
	$A^n_{3/2}$	−139±105	−15±19	18±28	10	15
	$A^n_{1/2}$	−19±87	2±5	−3±34	−49	7
$P_{11}(2055)$	$A^p_{1/2}$				−5	−18
$(20,1^+)2$	$A^n_{1/2}$				−1	6
$P_{13}(2060)$	$A^p_{3/2}$				−1.2	0.8
$(20,1^+)2$	$A^p_{1/2}$				−0.8	−10
	$A^n_{3/2}$				12	17
	$A^n_{1/2}$				−0.9	5.5

occur dominantly in the helicity-$\frac{3}{2}$ mode, leading to (see, e.g., Ref. 8)

$$A^N(Q^2=0)\approx -1 \ . \tag{3.3}$$

According to these two limiting cases one can thus expect that the helicity asymmetry starts at $Q^2=0$ from some negative value close to -1, then changes sign at $Q^2>0$ and finally reaches the value $+1$ in the region of high Q^2 where perturbative QCD becomes applicable.

For energy transfers ≤ 2 GeV the most prominent nucleon resonances excited in inelastic electron-nucleon scattering are the $\Delta(1232)$, $D_{13}(1520)$, and the $F_{15}(1680)$. The available experimental data are more complete and accurate for the electroproduction off proton than off the neutron. Nevertheless we shall also present results for neutrons since the following discussion will show that there are some significant differences between the two cases.

The helicity asymmetry of the $\Delta(1232)$ resonance has already been investigated in our previous paper:[4] Our photoproduction result (calculated from the values displayed in Table I) is in agreement with the experimental value $A^N\approx -0.5$ reflecting the fact that the excitation of this resonance is of purely magnetic type. This means also that we get for the E_{1+}/M_{1+} multipole ratio a value of -1.4%. Over the considered range of momentum transfers ($0\leq Q^2\leq 3$ GeV^2) the theoretical value of the $\Delta(1232)$ asymmetry remains approximately constant and no evidence is seen for a change of sign. This behavior also gained in the NRQM is in contradiction to predictions made, e.g., by Carlson[19] stating that the perturbative QCD regime (i.e., the value $A^N=1$) should already be reached at Q^2 values of a few GeV^2. However, since there are no precise electroproduction data available for this resonance this question cannot be definitively answered at present and remains a challenge for future experiments.

The situation looks quite different if one considers the next two prominent resonances: namely, the $D_{13}(1520)$ and the $F_{15}(1680)$. In Figs. 1 and 2 we display the helicity asymmetries A^p for these states calculated in the framework of the NRQM (dashed line) and with our ansatz (solid line). As one can see from these graphs, the results of our model are in close agreement with the experimental data over the whole range of Q^2 considered here, while the NRQM curves show no zero structure. It should be mentioned that the calculations of Refs. 20 and 21 in the framework of the NRQM show a better agreement with the experimental data but only on account of their different choice for the oscillator strength (about 30% larger than the value used in mass spectrum calculations, see the discussion in Ref. 4). The fact that A^p changes sign at rather low-momentum transfers $Q^2\approx 0.5$ GeV^2 indicates that this quantity is not necessarily a good test for the range of applicability of perturbative QCD. Indeed for such very low Q^2 one expects the nonperturbative effects to be still dominant (see, e.g., Ref. 22). It is interesting to note that the shape of the curves are quite similar for both resonances and that one observes a shift of the crossing point $A^p=0$ towards higher Q^2 as the resonance mass W grows. The slight decrease of A^p observed around 3 GeV^2 in Fig. 1 should not be taken too seriously since we are reaching here the limit of validity of our model. Indeed, the harmonic-oscillator wave functions cause the helicity amplitudes to drop very fast above $Q^2=2.5$ GeV^2 on account of the Gaussian shape (see Ref. 4). In contrast with the nonrelativistic case where all calculations can be done analytically the numerical accuracy chosen by us for the integration limits the significance of our results in this region to a few percent.

In Figs. 3 and 4 the helicity asymmetries of the $D_{13}(1520)$ and $F_{15}(1680)$ for a neutron target are shown. The F_{15} reaches the asymptotic limit (3.2) much faster and the zero is shifted to lower Q^2 values in comparison to the proton target case. The D_{13} shows a drastic different behavior above 1 GeV^2 than expected. Its neutron helicity asymmetry remains approximately zero indicating that the $A^n_{1/2}$ and $A^n_{3/2}$ are of the same size which illustrates again that we are far from the asymptotic QCD limit. Furthermore this should lead to different Q^2 dependencies in the polarization observables for the electroproduction off neutrons compared to protons.

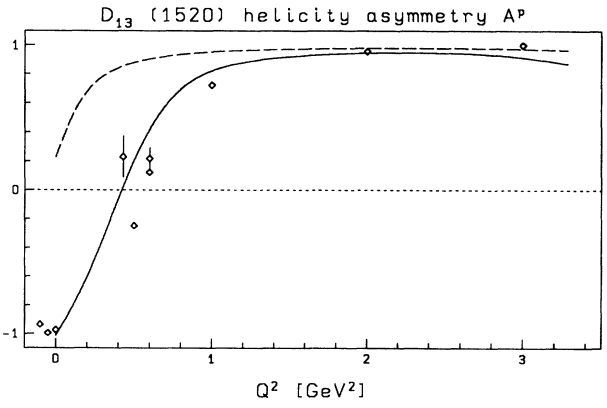

FIG. 1. The helicity asymmetry A^p for the $D_{13}(1520)$ resonance. The result of Ref. 4 (solid line) and the NRQM calculation including the configuration mixing of the wave functions (dashed line) are shown. Photoproduction data from Table I are displayed left from the point $Q^2=0$.

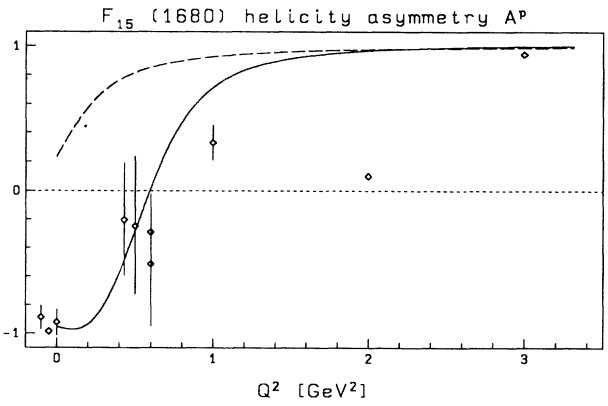

FIG. 2. The helicity asymmetry A^p for the $F_{15}(1680)$ resonance. Notation of curves and references of data points as in Fig. 1.

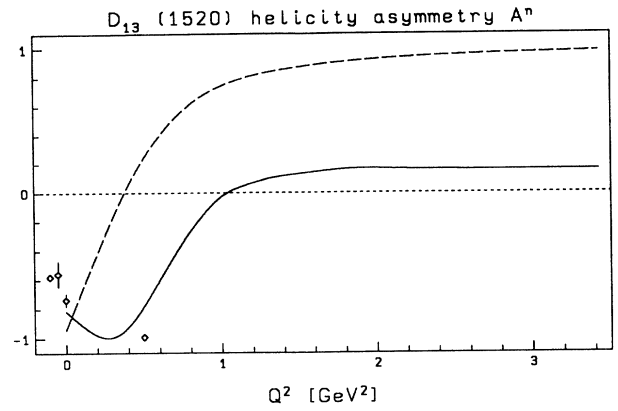

FIG. 3. The helicity asymmetry A^n for the $D_{13}(1520)$ resonance. Notation of curves and references for data points as in Fig. 1.

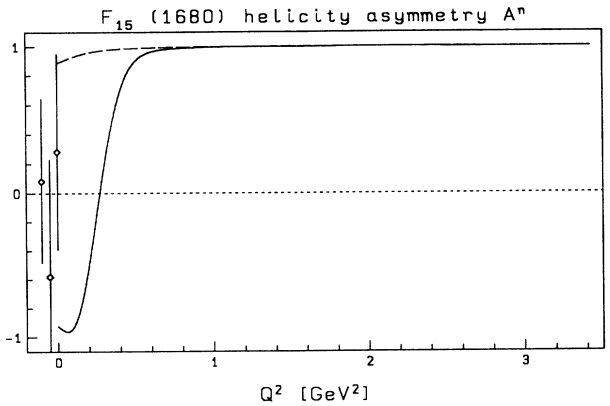

FIG. 4. The helicity asymmetry A^n for the $F_{15}(1680)$ resonance. Explanation of curves and references of data points as in Fig. 1.

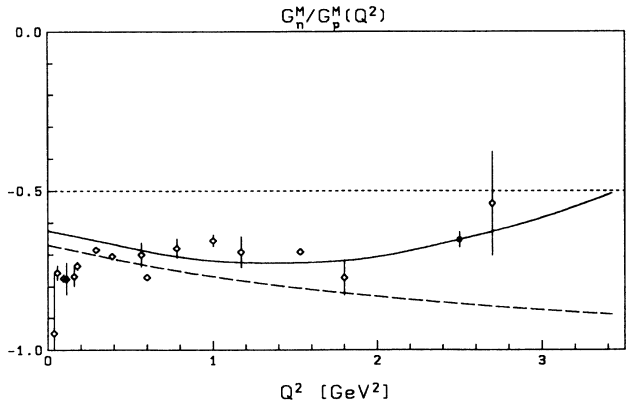

FIG. 5. The ratio of magnetic nucleon form factors as a function of Q^2. The result of Ref. 4 (solid line) and the NRQM calculation including the configuration mixing of the wave functions (dashed line) are shown. Experimental data points are gained for joint Q^2 from Refs. 24 (G_p^M) and 25 (G_n^M).

IV. ISOSPIN ASYMMETRIES

A further prediction made by perturbative QCD calculations and related to the hadron helicity conservation is connected with the Q^2 dependence of the magnetic nucleon form factors.[23] Indeed one expects that in the limit of asymptotic freedom the ratio of the neutron-to-proton magnetic form factors becomes

$$\frac{G_n^M(Q^2)}{G_p^M(Q^2)} \xrightarrow[Q^2\to\infty]{} \frac{e_d}{e_u} = -\tfrac{1}{2} + O(\ln Q^2) \ . \tag{4.1}$$

The underlying explanation is that the incoming high-Q^2 photon couples mainly to the constituent quark whose spin is parallel to that of the target nucleon (u quark in the proton case, d quark for the neutron target). On the other hand, at the photoproduction limit ($Q^2=0$) one gets the well-known result

$$\frac{G_n^M(Q^2=0)}{G_p^M(Q^2=0)} = \frac{\mu_n}{\mu_p} \approx -\frac{2}{3} \ , \tag{4.2}$$

which is characteristically reproduced by nearly all of the "QCD-motivated" models.

It is a major challenge for every model aiming to describe electromagnetic nucleon form factors at medium Q^2 to relate these two regimes. As one can see from Fig. 5, where we have displayed this ratio calculated for $Q^2 \leq 3$ GeV^2 with the NRQM (dashed line) and with our ansatz (solid line), both the experimental data and our result tend to reach the value of Eq. (4.1) at $Q^2 \approx 3$ GeV^2. Since by computing the ratio of form factors the Gaussian factors related to the choice of harmonic-oscillator wave functions (see Ref. 4) drop out, we may consider this result as a firm prediction of our model despite the fact that we are here at the limit of its confidential region. Whether the data also indicate that the perturbative regime starts already at $Q^2 \approx 3$ GeV^2 as has been argued, e.g., by Carlson,[19] however, is a question which can only be answered by more precise measurements of the magnetic neutron form factor at medium Q^2.

We consider now the first two resonances present in this energy region which are excited only in the helicity-$\frac{1}{2}$ mode, namely, the $S_{11}(1535)$ and the $P_{11}(1470)$. In Fig. 6 we display the $A^n_{1/2}/A^p_{1/2}$ ratio for the Roper resonance $P_{11}(1470)$ as a function of Q^2. The value $-\frac{2}{3}$ (dotted line) should occur in the NRQM if this state is a purely radial excitation of the nucleon. The inclusion of configuration mixing (dashed line) in the calculation does not change this conclusion very much. However, it is still experimentally unknown whether the electroproduction amplitudes lead to such a constant ratio. Our model calculations (see Fig. 6) show a dramatic variation of this ratio in the region $0 < Q^2 \leq 0.8$ GeV^2. There are several reasons for such anomalous behavior which contrast strongly with the ratio of magnetic nucleon form factors displayed in Fig. 5. At $Q^2 \approx 0$ the various relativistic corrections, neglecting the corrections due to the center-of-mass (c.m.) motion for a moment, are compensating each other to a very small net amount. Since at $Q^2=0$ the c.m. corrections are very small too—they reach their maximal strength around $Q^2 \approx 1.7$ GeV^2—the total $A^p_{1/2}$

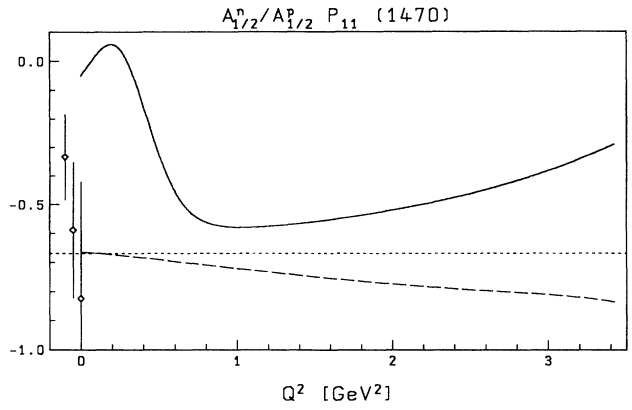

FIG. 6. The neutron-to-proton ratio of the $P_{11}(1470)$ helicity amplitudes. The result of our model presented in Ref. 3 (solid line), the NRQM calculation including the configuration mixing of the wave functions (dashed line), and the $SU(6)_W$ result (dotted line) are shown. Photoproduction data from Table I are displayed left from $Q^2=0$.

and $A^n_{1/2}$ amplitudes of the Roper resonance (see Fig. 7 and Fig. 13 of Ref. 4) show a very weak Q^2 dependence in this region. The strong decrease observed for their ratio from nearly zero down to the NRQM value in the region $Q^2 \leq 0.6$ GeV^2 should therefore be considered as a characteristic structure predicted by our model. Furthermore we want to stress that the existing experimental data at $Q^2=0$ with their large error bars do not strictly contradict our result (see Fig. 6). Finally the drastic Q^2 dependence of this ratio observed in our model might be relevant in polarization experiments and should help to clear up the questions about the existence and classification of the Roper resonance.

For the corresponding ratio of the $S_{11}(1535)$ resonance (see Fig. 8) we find a different behavior. In this case both the electric and magnetic terms of the interaction Hamiltonian contribute to the excitation amplitudes. Therefore we get an increase of the ratio for small Q^2 values. This fact again may be helpful for a separation between the P_{11} and the S_{11} resonances using the neutron-to-proton ratio of relevant observables.

As already mentioned above, using the spin-flavor

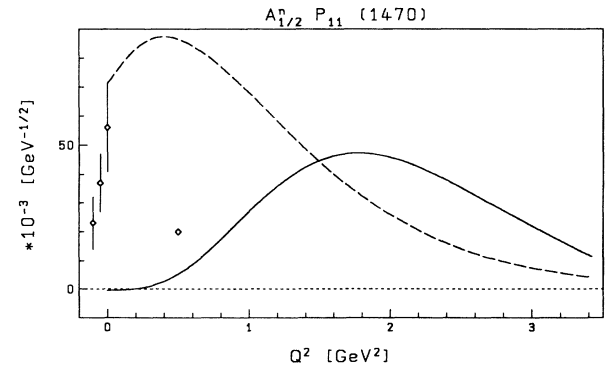

FIG. 7. The $A^n_{1/2}$ amplitude of the $P_{11}(1470)$ Roper resonance. Explanations of data and curves as in Fig. 6.

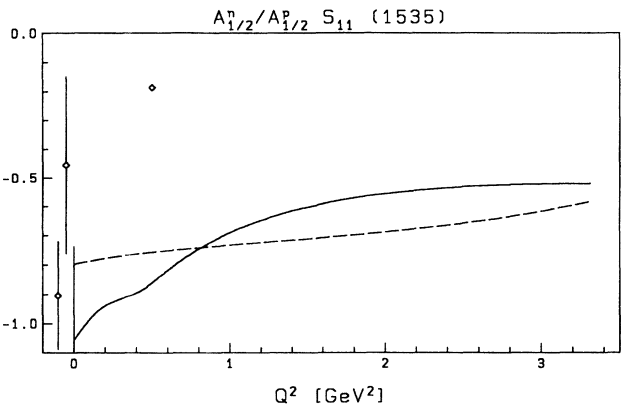

FIG. 8. The neutron-to-proton ratio of the $S_{11}(1535)$ helicity amplitudes. Explanations of data and curves as in Fig. 6.

structure of the wave functions and the single-quark transition ansatz (2.6) the helicity amplitudes (2.9) and (2.10) can be calculated in terms of the reduced matrix elements of the operators $\mathcal{A}$, $\mathcal{B}$, $\mathcal{C}$, and $\mathcal{D}$ (see, e.g., Ref. 8). For special combinations of helicity amplitudes one can build ratios in which these quantities drop out. As a prominent example one gets, for the $D_{13}(1520)$,[26]

$$\frac{A^p_{1/2}-(1/\sqrt{3})A^p_{3/2}}{A^n_{1/2}-(1/\sqrt{3})A^n_{3/2}}=-3\ . \tag{4.3}$$

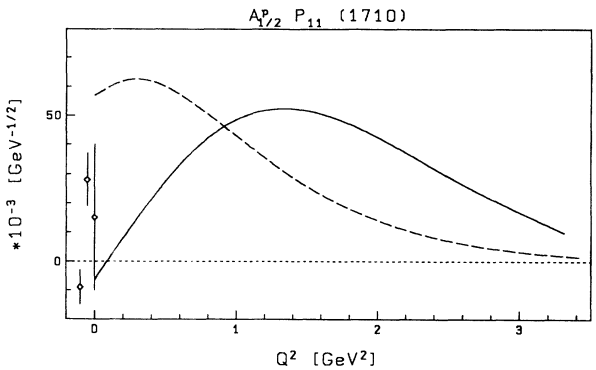

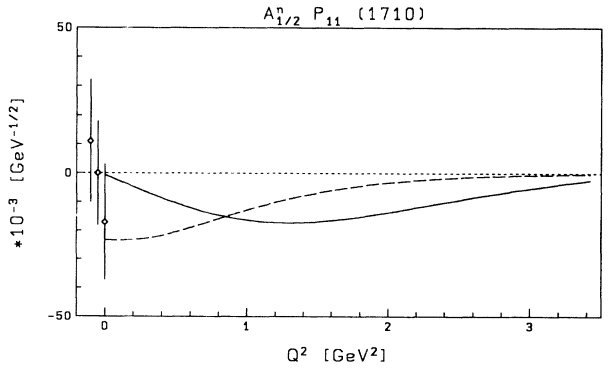

FIG. 9. The $A^n_{1/2}$ and $A^p_{1/2}$ amplitudes of the $P_{11}(1710)$ resonance. The dashed lines represent the nonrelativistic result including configuration mixing. For references of data see Table I.

It is often claimed in the literature that if the experimental data do not satisfy this "selection rule" this would be a serious flaw of the constituent quark model. However, considering the results of our model there are at least two reasons for deviations from this rule.

(1) Already in the framework of the NRQM, one has to include configuration mixing in the SU(6) baryonic wave functions in order to reproduce the correct mass splitting of the spectrum. These in turn give additional contributions to the photoproduction amplitudes and change the result of Eq. (4.3).

(2) Even more important are the multiquark operators which appear in a consistent derivation of the relativistic corrections to the NRQM. These operators displayed in (2.7b)–(2.7d) lead in general to a strong violation of the selection rule mentioned above.

To make the above statements more quantitative, we show below the values for the ratio (4.3) obtained with the NRQM including the configuration mixing of the wave functions (second column) and with our model (third column). Unfortunately the experimental error bars are so large that they do not allow us to make any

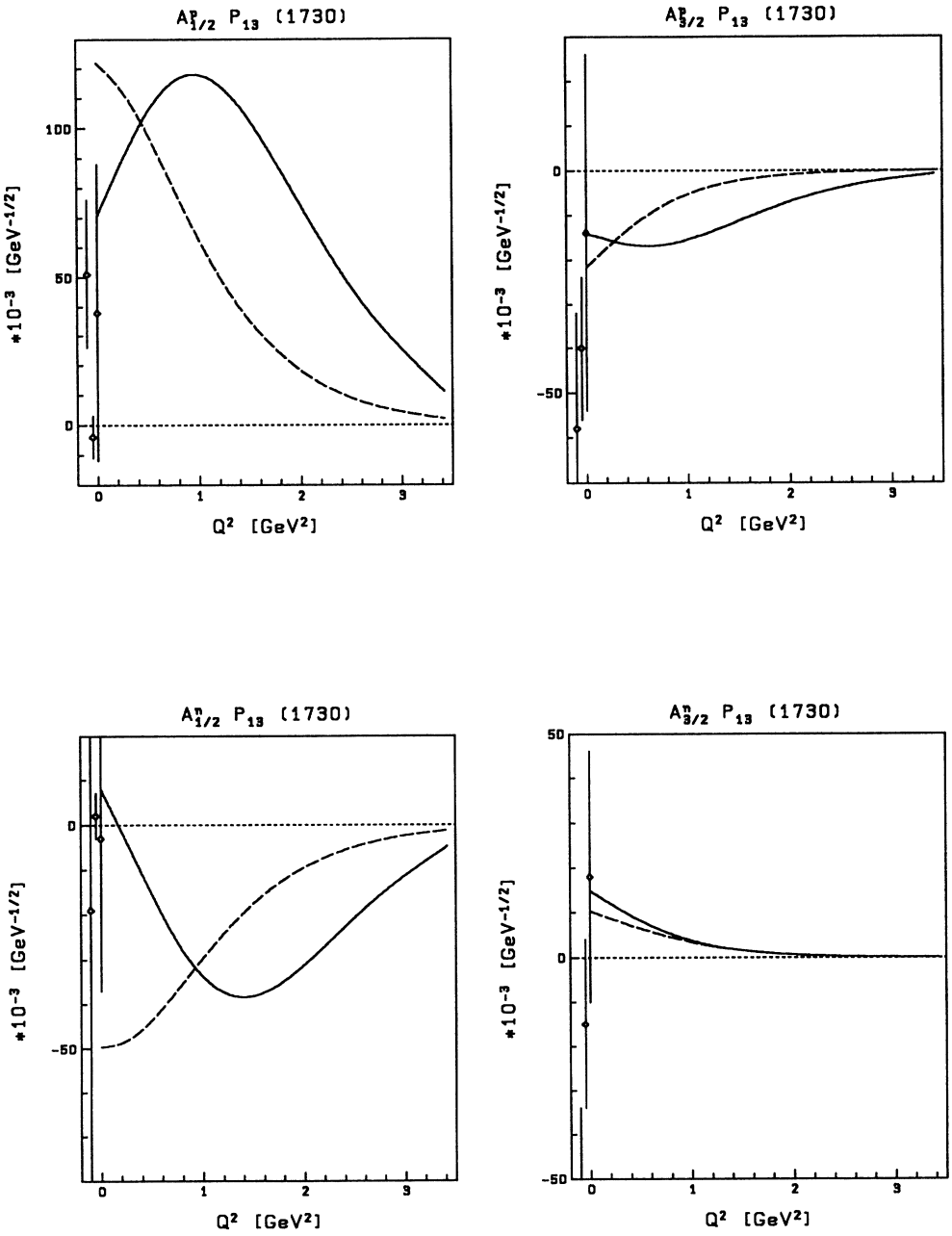

FIG. 10. Electroproduction amplitudes of the $P_{13}(1730)$ resonance. The dashed lines represent the nonrelativistic result including configuration mixing. The solid lines give the results of our model.

final conclusion. But this example shows that the inclusion of multiquark effects in the electromagnetic transition Hamiltonian changes drastically some of the predictions made on the basis of $SU(6)_W$ symmetry:

$SU(6)_W$	NRQM	Our model	Data
-3	-2.3	-1.35	-15 ± 15

V. ABOUT THE QUESTION OF HYBRID BARYONS

Calculations of the mass spectrum of hybrid baryons (i.e., baryons containing a "constituent" gluon in addition to the 3 quarks) in the framework of the MIT bag model[27] predict that the lowest-energy eigenstates should lie in the region between 1.5 and 2 GeV. On the other hand the results obtained with the NRQM for the photoproduction amplitudes of the $P_{11}(1470)$ (Roper resonance), $P_{11}(1710)$, and $P_{13}(1730)$ resonances[21] disagree with the experimental data. Therefore the interesting question arises if these resonances may be of a hybrid nature. In this case from the spin-flavor structure of their wave functions one would expect the following selection rules for the electroproduction amplitudes:[28]

$\|qqqG\rangle$ state	Photon amplitudes
P_{11}, P_{13}	$A_h^p=0$
$h=\frac{1}{2},\frac{3}{2}$	$A_h^n\neq0$

(5.1)

However, as can be seen in Table I, the relativistic corrections included in our model lead also to a strong suppression of the proton photoproduction amplitudes for these resonances. In contrast with the group-theoretic nature of the selection rule (5.1) this effect occurs in the framework of our model at the photoproduction point ($Q^2=0$) due to a mutual cancellation of the different terms contributing to these amplitudes.

Furthermore as shown in Fig. 9 our results for the $P_{11}(1710)$ are consistent with the data in both the neutron and proton case and show a significant Q^2 dependence. As in the case of the Roper resonance the photoproduction amplitudes are strongly reduced by the relativistic corrections in comparison to the NRQM. In this context we also refer the reader to a recent paper[29] where these amplitudes have been calculated with different radial wave functions.

In our opinion the situation for the $P_{11}(1470)$ Roper resonance is unclear with respect to this question (see the discussion in Sec. IV) but the experimental photoproduction data off protons clearly contradict the selection rule (5.1) as already stated in Refs. 28 and 26.

A further test case is the $P_{13}(1730)$ resonance. The experimental data are uncertain but seem to confirm the selection rule (5.1) at $Q^2=0$ (see Table I). However, our model reproduces these data quite accurately within the range of error bars. Furthermore our calculated electroproduction amplitudes displayed in Fig. 10 show again a strong Q^2 dependence. Especially the $A^p_{1/2}$ amplitude contradicts strongly the prediction issued from the hybrid model.

Obviously precise electroproduction data are needed to clarify the situation, but summarizing the previous discussion we consider our results as a strong hint in favor of a conventional explanation of the nature of these resonances.

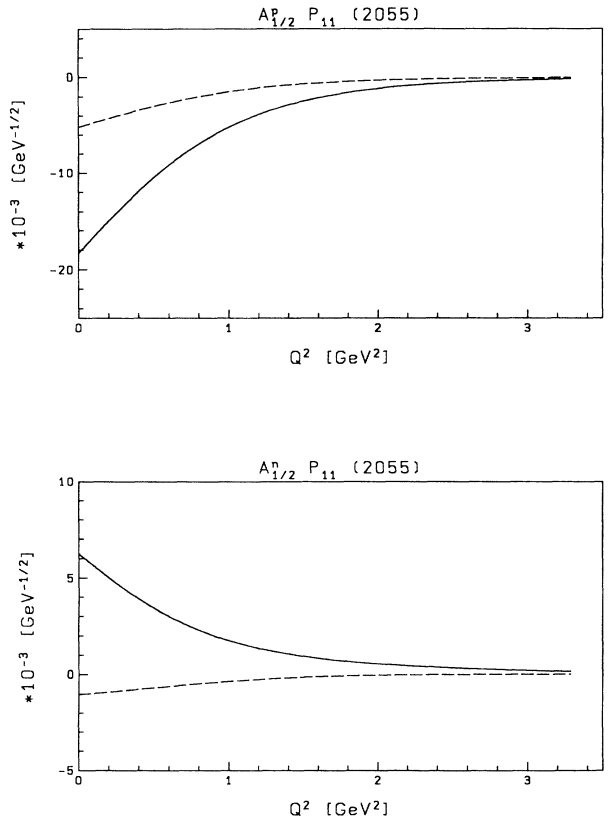

FIG. 11. The $A^n_{1/2}$ and $A^p_{1/2}$ amplitudes of the $P_{11}(2055)$ resonance. The dashed lines represent the nonrelativistic result including configuration mixing.

VI. ELECTROPRODUCTION OF $(20,1^+)$ RESONANCES

The NRQM predicts P-wave resonances in the $N=2$ band around 1800 MeV belonging to the $(20,1^+)$ multiplet. On account of the asymmetric space wave functions the πN decays of these resonances are strongly suppressed. This fact is in agreement with the presently available experimental data, where they have not been established until now. According to the calculations in the framework of the NRQM (Ref. 30) these resonances should decay dominantly in multipion channels such as $\pi\Delta,\omega N,\ldots$ (see also the review of Ref. 31). This has raised the question of how strongly they could be excited in the corresponding electroproduction reactions. There would be a good chance for establishing the missing resonances in these reactions if their radiative decay widths would be of equal size or enhanced relatively to the other contributing resonances. However, in the NRQM without configuration mixing their electroexcitation am-

plitudes are predicted to be exactly zero again due to the spin-flavor structure of the $(20,1^+)$ wave functions. But in our model the photoproduction results for helicity $\frac{1}{2}$ are strongly increased by the new relativistic terms (see Table I). On the other hand the configuration mixing of the wave functions, which is also a relativistic correction, has a comparatively smaller influence on the results. Figures 11 and 12 show that the electroproduction amplitudes vanish above 1 GeV^2 and that the photoproduction off neutrons of these resonances is somewhat enhanced in comparison to the proton case. Nevertheless, it seems to be hard to separate off these resonances from their more dominant companions even in high-precision experiments of vector-meson electroproduction.

VII. CONCLUSIONS

We have shown in this paper that relativistic corrections incorporated in a consistent manner into the nonrelativistic quark model lead to significant changes for the radiative transition form factors of nucleon resonances. These features are especially stringent in the case of the

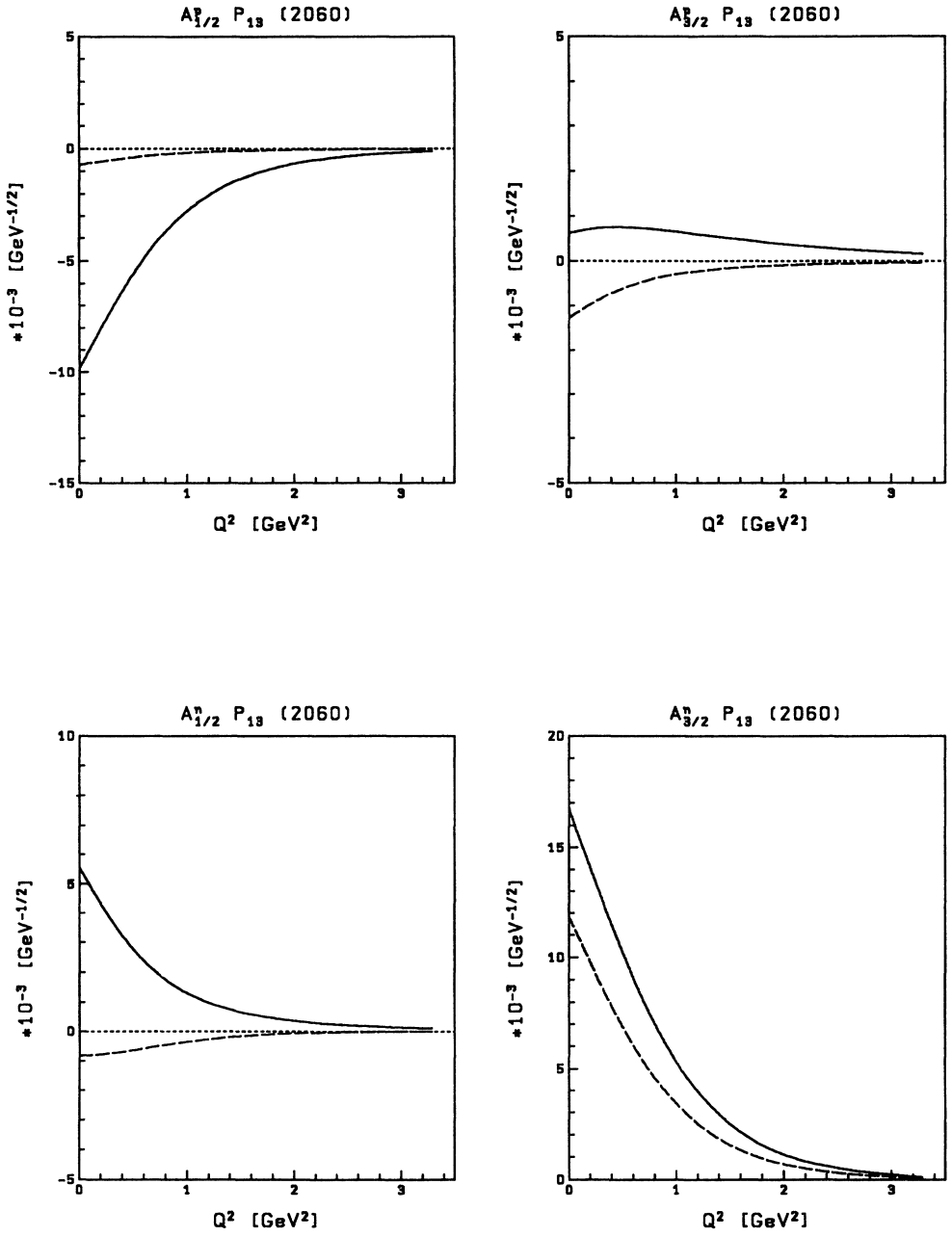

FIG. 12. Electroproduction amplitudes of the $P_{13}(2060)$ resonance. The dashed lines represent the nonrelativistic result including configuration mixing.

helicity asymmetries and isospin ratios presented in this paper. Our model leads here to some typical Q^2 structures reflecting the influence of the quark interaction potential and of the baryon recoil motion which should be tested in future experimental data against the predictions based on the single-quark-transition hypothesis. We would like to stress that all existing multipole analyses providing the "experimental" electroproduction data presented in the graphs relied mainly on this hypothesis. Future experimental data analyses should take into account the more general current operator (2.7a)–(2.7d).

Furthermore, we emphasized the importance of considering electroproduction experiments off both proton and neutron targets. These types of experiments are especially suited for giving new information about the various open questions in nucleon spectroscopy, e.g., concerning the nature of the P-wave states or the missing resonance problem. There are a lot of higher nucleon resonances which have not been considered in this paper nor in our preceding publication[4] (some additional amplitudes especially for the neutron target can be found in Ref. 32) but since the aim of this paper was to demonstrate only the characteristic features of relativistic corrections to the NRQM, we have restricted ourselves here to a special sample of nucleon resonances.

As we have already remarked the results of our calculations depend on the special choice of wave functions. We have used the set of harmonic-oscillator states from Ref. 12 which obviously are not eigenstates of our model Hamiltonian. The dependency of our results on the quark-quark interaction potential observed in Ref. 4 indicates that one should calculate simultaneously the mass spectrum, the wave functions, and the transition amplitudes of baryons in the framework of the same relativized quark model. Nevertheless, since in the amplitude ratios considered in this paper the main influence (Gaussian factor) of the harmonic-oscillator wave functions cancels out, the presented results give some deeper insight into the nucleon resonance structure from the quark-model point of view. However, further investigations should concentrate on the question to find suitable wave functions which take also into account the features related to the internal spin structure of the nucleon as discussed in the literature (e.g., Ref. 33).

Note added. After submitting this paper for publication we received papers by Weber and Konen[34,35] presenting results for the $P_{11}(1470)$ and $S_{11}(1535)$ transition amplitudes obtained with a relativistic constituent quark model and a paper by Close and Li[36] investigating QCD mixing effects on the electroproduction of baryon resonances in the framework of the constituent quark model.

---

*Electronic address: UNP010@DBNRHRZ1 bitnet.

[1]J. L. Rosner, in *Techniques and Concepts of High Energy Physics,* proceedings of the NATO Advanced Study Institute, St. Croix, Virgin Islands, 1980, edited by Th. Ferbel (NATO ASI Series B: Physics, Vol. 66) (Plenum, New York, 1980).

[2]N. Isgur, in *The New Aspects of Subnuclear Physics,* proceedings of the XVI International School, Erice, Italy, 1978, edited by A. Zichichi (Subnuclear Series, Vol. 16) (Plenum, New York, 1981), p. 107.

[3]M. Warns, H. Schröder, W. Pfeil, and H. Rollnik, Z. Phys. C **45**, 613 (1990).

[4]M. Warns, H. Schröder, W. Pfeil, and H. Rollnik, Z. Phys. C **45**, 627 (1990).

[5]F. E. Close, *Introductions to Quarks and Partons* (Academic, New York, 1978).

[6]H. Rollnik, in *Electromagnetic Interactions and Field Theory,* proceedings of the XIV Winter School, Schladming, Austria, 1975 [Acta Phys. Austria Suppl. **XIV**, 5 (1975)].

[7]H. J. Melosh, Phys. Rev. D **9**, 1095 (1974).

[8]F. Foster and G. Hughes, Rep. Prog. Phys. **46**, 1445 (1983).

[9]C. Avilez and G. Cocho, University of Mexico Report No. IFUNAM 77-06, 1977 (unpublished).

[10]L. L. Foldy and S. Wouthuysen, Phys. Rev. **78**, 29 (1950).

[11]J. D. Bjorken and S. D. Drell, *Relativistic Quantum Mechanics* (McGraw-Hill, New York, 1964).

[12]N. Isgur and G. Karl, Phys. Rev. D **18**, 4187 (1978); **19**, 2653 (1979); N. Isgur, G. Karl, and R. Koniuk, *ibid.* **25**, 2394 (1982).

[13]D. Gromes, Heidelberg University Report No. HD-THEP-89-17, 1989 (unpublished).

[14]Particle Data Group, Rev. Mod. Phys. **48**, 5157 (1976).

[15]I. Arai and H. Fujii, Nucl. Phys. **B194**, 251 (1982).

[16]N. Awaji *et al.*, in *Lepton and Photon Interactions at High Energies,* proceedings of the 10th International Symposium, Bonn, Germany, 1981, edited by W. Pfeil (Physikalisches Institut, Universität Bonn, Bonn, 1982), p. 352.

[17]R. L. Crawford and W. T. Morton, Nucl. Phys. **B211**, 1 (1983).

[18]C. E. Carlson, in *Excited Baryons 88,* proceedings of the Topical Workshop, Troy, New York, 1988, edited by G. Adams, N. C. Mukhopadhay, and P. Stoler (World Scientific, Singapore, 1988).

[19]C. E. Carlson, Phys. Rev. Lett. **58**, 1308 (1987).

[20]L. A. Copley, G. Karl, and E. Obryk, Nucl. Phys. **B13**, 303 (1969).

[21]R. Koniuk and N. Isgur, Phys. Rev. D **21**, 1868 (1980).

[22]N. Isgur and C. H. Llewellyn Smith, Nucl. Phys. **B317**, 526 (1989).

[23]F. E. Close and A. W. Thomas, Phys. Lett. B **212**, 227 (1988).

[24]D. Krupa *et al.*, J. Phys. G **10**, 455 (1984).

[25]W. Bartel *et al.*, Nucl. Phys. **B59**, 429 (1973); S. Rock *et al.*, Phys. Rev. Lett. **49**, 1139 (1982).

[26]F. E. Close, in *Research Program at CEBAF,* proceedings of the 1988 Summer Workshop (CEBAF, Newport News, 1989).

[27]T. Barnes and F. E. Close, Phys. Lett. **123B**, 89 (1983).

[28]T. Barnes and F. E. Close, Phys. Lett. **128B**, 277 (1983).

[29]Fl. Stancu and P. Stassart, Phys. Rev. D **41**, 916 (1990).

[30]N. Isgur, in *Electron and Photon Interaction at Intermediate Energies,* edited by D. Menze, W. Pfeil, and W. Schwille (Springer Lecture Notes in Physics, Vol. 234) (Springer, Berlin, 1977).

[31]D. Menze, in *Excited Baryons 88* (Ref. 18).

[32]H. Schröder, Diploma thesis BONN-IR-85-09, Bonn University, 1985.
[33]H. Fritzsch, Phys. Lett. B **229**, 122 (1989), and references therein.
[34]H. J. Weber, Phys. Rev. C **41**, 2783 (1990).
[35]W. Konen and H. J. Weber, Phys. Rev. D **41**, 2201 (1990).
[36]Z. Li and F. E. Close, this issue, Phys. Rev. D **42**, 2207 (1990).